

Journal of Engineering Research

ELECTROMECHANICAL STRESSES ON POLLUTED POLYMERIC INSULATORS

Reinaldo Corrêa Leite

Universidade Federal do Pará, Belém-Pará-
Brasil

Filipe Matheus do Rosário Menezes

Universidade Federal do Pará, Belém-Pará-
Brasil

All content in this magazine is licensed under a Creative Commons Attribution License. Attribution-Non-Commercial-Non-Derivatives 4.0 International (CC BY-NC-ND 4.0).



Abstract: This work develops a Finite Element model for evaluation of the electric field distribution and the electromechanical stress tensor (EST) caused by the flow of the leakage current on an electrolytic pollution layer on the surface of a polymeric insulators. The effect of the EST is evaluated over the insulator surface and on two types of defects, namely: cracks on the sheath/shed transition region and on a void inside the polymeric housing. The simulations show stresses of the order of 11 Pa on the crack tip and that voids are stretched by the EST. Based on these results, the model can be used to estimate the effects of EST on polymeric insulator housing.

Keywords: Polymeric Insulators, Simulation, Leakage Current, Electromechanical Stresses.

INTRODUCTION

Polymeric or composite insulators have been used on transmission lines since 1960s when General Electric developed the first insulators of this type [1]. Their reduced weight, mechanical resistance, electrical supportability and hydrophobicity are superior when compared to their ceramic counterparts and such features made them popular around the world. However, the weakness of fiber glass and polymer composites in corrosive environments affects the polymeric insulators performance and useful life [2].

The corrosive environment enables the occurrence of brittle fracture which is a failure mode that occurs when the Fiber Reinforced Plastic rods enters in contact with nitric acid produced by corona discharges originated from the dry band phenomenon as described in [3] and collapses even when the applied mechanical load in service is not to large [5]. The brittle fracture is the most familiar abnormal fracture of composite insulators and has been studied for at least two decades giving rise to a vast literature about this subject as can be seen in the references [2]-[8].

The nitric acid (NO_3) is formed by the reaction of ozone and the nitrogen in the atmospheric air, and comes in contact with the FRP rod when the polymeric housing degrades forming crazes that leads the insulator core exposed. The material that forms the polymeric housing is silicone rubber, which has as base material polydimethylsiloxane (PDMS) in which the main chain is Si-O-Si and side chain is Si- CH_3 . Figure 1, extracted from [9], shows the structure of PDMS. As the polymeric material is organic, it is sensitive to environmental conditions leading the insulator housing material to degrade with time. Therefore, it is necessary to understand how the operational conditions affect service performance of the insulators in order to make the transmission system reliable and safe.

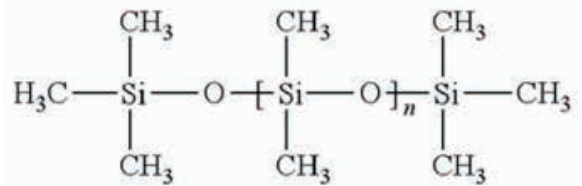


Fig. 1. Chemical structure of PDMS polymeric compound. Reference [9].

The degradation of the insulator housing is investigated since the 1990s. Fourmigue et al. [10] carried out an investigation to assess the performance of silicone rubber (SiR) and EPDM under natural and accelerated conditions. The researchers found several definitive changes in surface properties such as increasing hardness, roughness and surface oxidation of the tested insulators in both accelerated and natural tests. Gorur et al. [11] used analytical techniques such as Fourier Infra-Red Transform Spectroscopy (FTIR), Energy Dispersive X-Ray (EDX), Analysis X-Ray Diffraction (XRD) and surface roughness measurements to investigate the permanent changes in the material that lead to progressive degradation in long term run.

The chemical and morphological changes in the PDMS/ATH system in polymeric insulators subjected to dry band arcing or high temperatures were described in [12]. The study showed that the PDMS/ATH system was prone to tracking phenomenon and lead to dielectric breakdown when subjected to standardized tracking test.

The effect of pollution on the surface degradation of silicone rubber insulators was investigated in [14], where the researchers focused on the effects of environmental aging during tracking process on High Temperature Vulcanizing (HTV) silicone rubber insulators for outdoor applications. The insulators surface was polluted to analyze the leakage current magnitude and arcing effect on aging. The authors also investigated the physicochemical properties to understand the crystalline nature and crystal size at eroded region of each sample by means of XRD analysis and FTIR spectroscopy. The FTIR analysis showed a reduction of the Si-O rocking vibrations in aged samples indicating, according to the authors, that the aging of the polymeric sample before the tracking test considerably affects Si-CH₃ and Si-O bond in the polymeric chain. The investigations also revealed that the tracking on thermal aged samples showed that the deformation in the Si-O and Si-CH₃ bond had resulted in higher erosion of polymeric material.

The result of tracking on polymeric insulators was also addressed on [15] where a multi-stress aging study was carried out to evaluate long term reliability of SiR insulators subjected to environmental stresses such as humidity, temperature, UV radiation and electrical stress. The changes in physical, chemical and mechanical properties of silicone rubber material due to applied stresses were explored by means of FTIR spectroscopy, EDX, TGA, XRD and tensile strength assessment. The FTIR spectroscopy

found a huge reduction in peak at 1008 cm⁻¹ confirming the main chain bond breakage leading to depolymerization and material degradation after a 1000 h aging.

The integrity of a polymeric structure is held by two types of bonds: the covalent bonds between atoms and Van der Waals forces between molecules. The severance of either bonds leads to chain scission that evolves to a change in mechanical properties and at last in material fracture [16],[17]. When a stress is applied to a polymer sample a disproportionate amount of load is distributed in certain chain segments, which can be sufficient to exceed the bond strength, this is especially true for amorphous polymers like SiR [17]. In addition, beside mechanical forces due to conductor weight, polymeric insulators are subjected to high electric fields originated from the applied voltage, and it is well known that dielectrics deform when subjected to a voltage, especially elastomers like SiR. For such dielectrics, this effect can be produced by either electrostrictive stresses and Maxwell stress [18]. Therefore, if such stresses are capable to overcome the forces that keep the integrity of the polymeric structure by severing the bonds, this can lead to chain scission, i.e., a fracture at atomic level and at least to material separation as proposed by Lewis in [18] creating a crack on the SiR sheath.

This paper develops a Finite Element Model (FEM) to evaluate the electromechanical stress due to the electric field produced by the leakage current over the surface of a distribution SiR insulator. It is structured in the following way: Section II is a brief review of stresses on solid dielectrics. Next, Section III deals with the modelling of the insulator and Section IV discusses the simulation results.

ELECTRO MECHANIC FORCES ON A SOLID DIELECTRIC IN AN ELECTROSTATIC FIELD

An overhead insulator of any type of material is subjected to electrical and mechanical stresses. As these stresses are the result of the electromechanical forces exerted in the field upon the charges and current induced on the insulator or upon the neutral matter that composes the insulator material [18], this section brings a brief review of the behavior of the stresses that appear on an insulator, starting with an analysis of continuum mechanics and evolving to a description of the forces and stresses due to the electric field.

A. A REVIEW OF FORCES CONTINUUM MECHANICS

Consider a solid in static equilibrium under a system of applied forces, by means of an isolated volume element V , surrounded by a closed surface S , inside the insulator sheath, as shown in Figure 2.

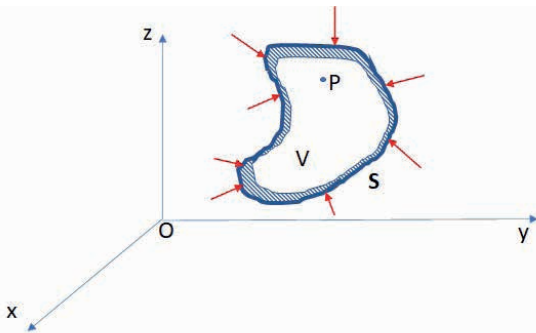


Fig. 2. Region V inside the insulator sheath bounded by a surface S under stress. Reference [18].

If the body is in equilibrium it means that all its parts are in equilibrium, so for the volume depicted on Figure 2, the following condition must be attained [19].

$$\nabla \cdot \mathbf{T} + \mathbf{f}_{ext} = 0 \quad (1)$$

Equation (1) states that the resultant force over the matter enclosed by S must be zero. The divergent term on Equation (1) stands for the surface forces that are exerted by elements of matter just outside the volume boundary on elements neighboring the surface S inside the volume. The term \mathbf{f}_{ext} represents the body or volume forces such as gravity or electric force that are external to the volume. \mathbf{T} has components that are normal pressures or stress and tangential shears and is called the stress tensor. This equation is solved for the special case where the material is linear elastic [18],[19]. Another condition is the continuity of the stress tensor across a stationary boundary between two materials, which corresponds to Equation (2).

$$\mathbf{n}_1(T_2 - T_1) = 0 \quad (2)$$

In Equation (2) T_1 and T_2 are the stress tensor in materials 1 and 2, respectively and \mathbf{n}_1 is the normal unit vector that points out from the volume that contains material 1. This condition originates a force that acts on the boundary between the two media formed by material 1 and 2 and is illustrated on Figure 3.

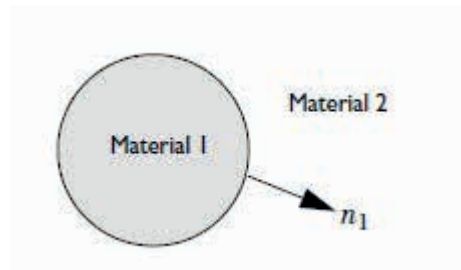


Fig. 3. Representation of the continuity of stress tensor across a boundary between two media. Reference [19].

Therefore, in the polymeric insulator case, material 1 can be regarded as the SiR sheath and material 2 is the pollution layer. As the insulator is subjected to an electric

field, the applied stress can be resolved in two components: one due to the electromagnetic field and the other is the mechanical stress tensor as shown in Equation (3).

$$T = T_{EM} + \sigma_M \quad (3)$$

B. FORCE ON A SOLID SURROUNDED BY AIR

Referring again to the enclosed volume V surrounded by a closed curve S forming a boundary in which there is an isotropic dielectric under elastic stress, surrounded by air. On this boundary, the following equations hold for the balance of forces on the solid.

$$\nabla \cdot T_1 + \mathbf{f}_{ext} = \mathbf{f} = 0 \quad (4)$$

$$\mathbf{n}_1(T_2 - T_1) + \mathbf{g}_{ext} = \mathbf{t} = 0 \quad (5)$$

Where \mathbf{g}_{ext} is an external boundary force representing a reaction force from the matter outside the volume V . The total force is calculated by applying the condition of translational equilibrium [18].

$$\int \mathbf{f} dv + \int \mathbf{t} dS = 0 \quad (6)$$

In Equation (6) \mathbf{f} and \mathbf{t} are respectively, the distributed force density per unit volume and the force exerted by the matter outside the surface S , on a unit area [18]. Substituting (4) and (5) into (6).

$$\int (\nabla \cdot T_1 + \mathbf{f}_{ext}) dv + \int (\mathbf{n}_1(T_2 - T_1) + \mathbf{g}_{ext}) dS = 0 \quad (7)$$

Expanding and rearranging Equation (7).

$$\int \nabla \cdot T_1 dv - \int \mathbf{n}_1 T_1 dS + \int \mathbf{f}_{ext} dv + \int \mathbf{n}_1 T_2 dS + \int \mathbf{g}_{ext} dS = 0 \quad (8)$$

Applying the Gauss' theorem to the first to terms of Equation (8).

$$\int \nabla \cdot T_1 dv - \int \mathbf{n}_1 T_1 dS = 0 \quad (9)$$

The integrals of \mathbf{f}_{ext} and \mathbf{g}_{ext} , when added, give the external force shown in Equation (10)

$$\mathbf{F} = \int \mathbf{f}_{ext} dv + \int \mathbf{g}_{ext} dS - \int \mathbf{n}_1 T_2 dS \quad (10)$$

This external force balances the force produced by the stress inside the volume keeping the body in equilibrium. If the external force by some means is removed, the solid begins to giving rise to a strain [19].

C. ELECTROMAGNETIC STRESS TENSOR

Supposing again the unit volume V enclosed by the closed surface S , with an isotropic dielectric inside the volume V submitted to an electrical stress. Assuming the properties of the dielectric are continuous across the surface and all the interior points. The total force exerted by on the matter and charge within S is given by Equation (10), as seen before. As stated by Equation (3) the total stress can be divided into two components one electromechanical and other mechanical. Disregarding the mechanical component, the last term in Equation (10) is due only to the electrical stress.

$$T_2 = T_{EM} \quad (11)$$

For air or vacuum, the electrical stress tensor is given by.

$$T_2 = -pI - \left(\frac{\epsilon_0}{2} \mathbf{E} \cdot \mathbf{E} + \frac{1}{2\mu_0} \mathbf{B} \cdot \mathbf{B} \right) I + \epsilon_0 \mathbf{E} \cdot \mathbf{E}^T + \frac{1}{\mu_0} \mathbf{B} \cdot \mathbf{B}^T \quad (12)$$

In Equation (12) p accounts for the air pressure, I is the identity 3-by-3 tensor, \mathbf{E}

and \mathbf{B} are 3-by-1 vectors representing the electric and magnetic fields [19]. Using the constitutive relations $\mathbf{D}=\epsilon_0\mathbf{E}$ and $\mathbf{B}=\mu_0\mathbf{H}$, Equation (12) can be rewritten as:

$$T_2 = -pI - \left(\frac{1}{2}\mathbf{E} \cdot \mathbf{D} + \frac{1}{2}\mathbf{B} \cdot \mathbf{H}\right)I + \mathbf{E} \cdot \mathbf{D}^T + \mathbf{H} \cdot \mathbf{B}^T \quad (13)$$

Thus, for a solid surrounded by air, as is the case for the polymeric transmission line insulator, the total force is computed by Equation (14).

$$\mathbf{n}_1 T_2 = -p\mathbf{n}_1 - \left(\frac{1}{2}\mathbf{E} \cdot \mathbf{D} + \frac{1}{2}\mathbf{B} \cdot \mathbf{H}\right) \mathbf{n}_1 + (\mathbf{n}_1 \mathbf{E}) \cdot \mathbf{D}^T + (\mathbf{n}_1 \mathbf{H}) \cdot \mathbf{B}^T \quad (14)$$

Therefore, \mathbf{n}_1 is unit vector normal to the surface, pointing out the solid and this expression can be used to calculate the total force as an integral of the stress tensor over the boundary the elapses the solid. A thorough demonstration of the obtention of the electrical stress tensor can be found in references [18], [20] and [21]. In these references a merge of material theory, thermodynamics, continuum mechanics and electromagnetic field theory are used.

DISTRIBUTION OF ELECTROMAGNETIC STRESS TENSOR IN A POLYMERIC INSULATOR

Polymeric insulators installed on aerial transmission and distribution lines are composed by the metal end fittings, the polymeric SiR sheath and FRP core. Besides that, insulators installed near coastal or industrial areas, are subjected to pollution in the form of salt deposit (coastal area) or dirt originated from industrial processes [23]. Therefore, the FEM analysis has to consider

a solid model composed by the insulator (material 1), the pollution layer (material 2) surrounded by a third material which is the air, that in many applications can be approximated by the vacuum [19]. Thence, the equations developed in the last section will be used to model the distribution of electromagnetic field and the stress tensor on a polymeric insulator.

A. INSULATOR AND POLLUTION LAYER MODELING

The polymeric insulator chosen for the simulations is a 138 kV HTV-SiR insulator which dimensions are listed on Table 1. The pollution layer on an insulator is accumulated on its surface by two different processes: dry deposition and occult deposition. The first process occurs when the deposits settle on both top and bottom insulator surfaces. The second process happens when rain, fog, etc. precipitates over insulator surface and creates a conductive electrolyte [22]. For the pollution layer, a thickness of 1 mm was considered as suggested in [25]. This layer represents the accumulated pollutants, as shown on Figure 4. The vast majority of pollutants accumulated over the insulator surface are salts, that under influence of moisture are easily dissociated giving rise to a conductive path through which flows the leakage current (LC).

Height (mm)	1175
Core Diameter (mm)	27
SiR Thickness (mm)	3
Number of Sheds	43
Leakage Distance (mm)	3735
Shed Diameter (mm)	220/190
Voltage Class (kV)	138

Table 1: Dimensions and Characteristics of the Polymeric Insulator.

The distribution of the pollution layer is based on the Equivalent Salt Deposit

Density (ESDD) as defined in [26]. The pollution accumulation on insulators is strongly influenced by the concentration of pollutants on air; by the mass flow rate past insulator surface; by the orientation of the surface relative to the wind and air flow patterns around the insulator profile and capture efficiency of the surface material and condition [25]. Studies carried out by Hall and Mauldin [27] compared the three forces that appear on a salt particle: the gravitation force, the viscous force and a dielectrophoresis force from field induced dipoles in the dielectric particle subjected to an electric field, this last force directs the particle to regions of maximum electric field. When the particles move near zones where air velocity is near zero, the dielectrophoresis force becomes dominant and the particles are attracted to the surface where the electric field is more intense. On the other hand, soft insulator surfaces such as those of insulators composed of silicone, attract more pollution than their ceramic counterparts because of the presence of light molecular weight oil that captures and encapsulate pollutants particles, which leads to a significant difference in washing efficiency, causing a difference between top and bottom pollution layer [22]. In the model, this difference is attained by considering a different conductivity for the top and bottom layers as proposed in [25]. The material properties are listed on Table 2.

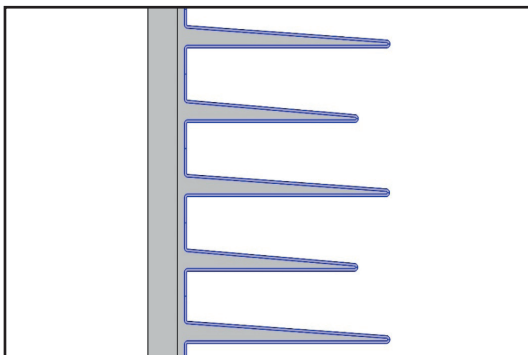


Fig. 4 - Pollution layer model

Material	Conductivity σ (S/m)	Relative Permittivity (ϵ)
Silicone Rubber	10^{-12}	4
FRP Core	10^{-14}	6,5
Pollution Layer on Top Shed	$6,42 \times 10^{-3}$	80
Pollution Layer on Bottom Shed	$12,85 \times 10^{-3}$	80
End Fittings	$5,9 \times 10^7$	1
Air	10^{-20}	1

Table 2: Properties of the materials used on each insulator component.

The end fittings are represented as a Dirichlet boundary condition by an imposed potential of 138 kV (AC-60 Hz) at the insulator conductor end and 0 kV at the ground end. The mesh used for the Finite Element Method (FEM) simulation is shown in Figure 5. The insulator was simulated using a 2D axisymmetric geometry due to its symmetry. The simulation domain is a hemisphere used to create an air volume around the insulator.

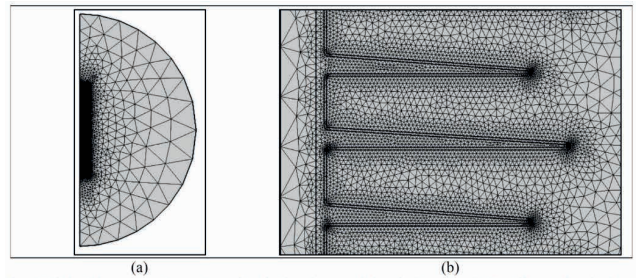


Fig. 5: Finite Element mesh (a) Covering the insulator and the air domains (b) Detail near the sheds.

B. DEFECTS MODELING

Cracks and voids are the two types of defects modeled to analyze the impact on the distribution of electric field and electromechanical stresses and were modeled using 2D geometry. The cracks are represented as a triangular cutout, 1 mm deep, in the surface of the SiR casing at the intersection of the shed and the sheath, as shown in Figure 6. This representation is chosen because the

actual insulators taken out of service after the line inspections showed cracks in that region as seen in Figure 7.

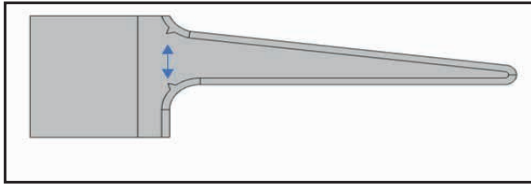


Fig. 6 – Crack model on the silicone rubber housing of the insulator

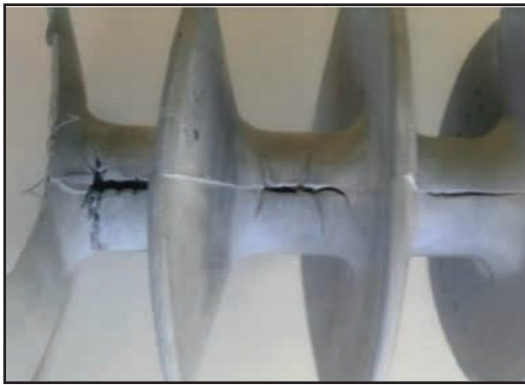


Fig. 7 – Crack on an actual insulator taken from service.

Voids can appear in the polymer if a tension, high enough, rearranges the polymer's molecular chain, forming fibrils like bundles. The spatial incompatibility between these chains allows the appearance of voids as shown in Figure 8, the process that leads to void formation usually starts due to the occlusion of inorganic particles in the polymer during the manufacturing process [17]. The void is represented within the SiR casing as a circular cavity of 1mm diameter. This geometry is chosen due to the studies carried out by [28] and [30] on the formation of faults in dielectric materials. The cavity added to the insulator model is shown in Figure 9 and is filled with air.

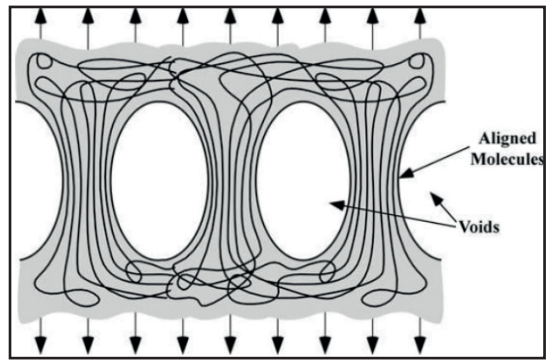


Fig. 8 – Voids formed between fibrils in polymers [17].

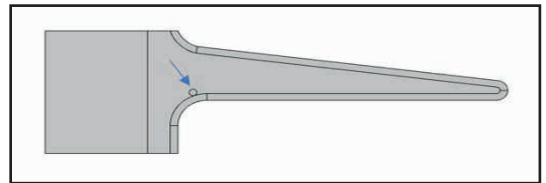


Fig. 9 – Circle filled with air inside the polymeric housing.

RESULTS AND DISCUSSION

A 138 kV-60 Hz voltage is applied to the lower end of the insulator while the upper end is grounded as found on actual insulators installed on transmissions lines. This procedure was done for both situations: for the insulator under clean conditions and for the insulator under the pollution conditions, already described, in order to compare the increase in leakage current and its consequences.

A. DISTRIBUTION OF THE ELECTRIC FIELD ALONG THE INSULATOR

The electric field is calculated for two situations: first for a clean insulator (without a pollution layer) and then for a polluted insulator. The strength of the electric field inside a conductive medium is related to the current density and the electrical conductivity of the medium: $J = \sigma E$, which is the punctual form of Ohm's Law that is valid for ionized solutions [29], such as the pollution layer.

There is significant variation in the electric field on the silicone rubber surface in both situations. In the clean insulator, as can be seen in Figure 10.a, the electric field has higher magnitude values at its ends and which reduce to almost zero in the central part of the insulator. On the other hand, the polluted insulator has another configuration for the electric field, shown in Figure 10.b, without elevations at its terminals, but with the greatest field strength close to the curvatures at each transition from each sheath to the shed, with levels around 2.5 to 3 kV / cm and with this pattern throughout the equipment. Due to the change in the conductivity of the medium between the upper and bottom layers of the pollutant, discontinuities arise in the field module over the SiR.

This change occurs because the pollution layer becomes a resistive conductive path and allows a greater leakage current to flow across the surface, increasing the current density and also the electric field inside the sheds. The calculated current density for the two insulator conditions is shown in Figure 11. This figure shows an increase in current density to 0.6 kA / m² in the SiR when the polluted insulator is compared to the clean insulator, reflecting the increase in current of surface leakage indicated in figure 12.a for the clean insulator (in μ A) and in figure 12.b for the polluted insulator (in mA). As the electric field is proportional to the current density, the new field configuration is clarified.

B. DISTRIBUTION OF MAXWELL STRESS TENSOR ALONG THE INSULATOR

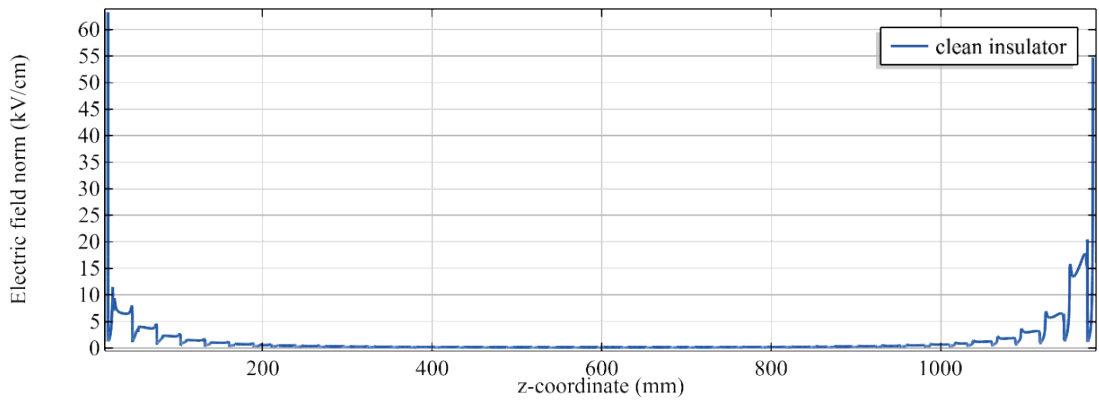
Maxwell's electromechanical tensor was evaluated in the structure to verify the forces acting on the surface of the polymeric housing. In this simulation, the force is exclusively electrical. like the electric field, the tensor behaves in a peculiar way in the

two simulated cases. In clean conditions, the electromechanical efforts are concentrated only and intensively at the vicinity of the terminals, see figure 13.a, while along the length of the equipment the tensor values are practically nil. On the other hand, in the polluted condition, the efforts are more distributed along the device, mainly inside the sheds, as shown in Figure 13.b. In both situations, the behavior is very similar to the profile of the electric field already presented, this is due to the relationship between these two quantities through equation 14.

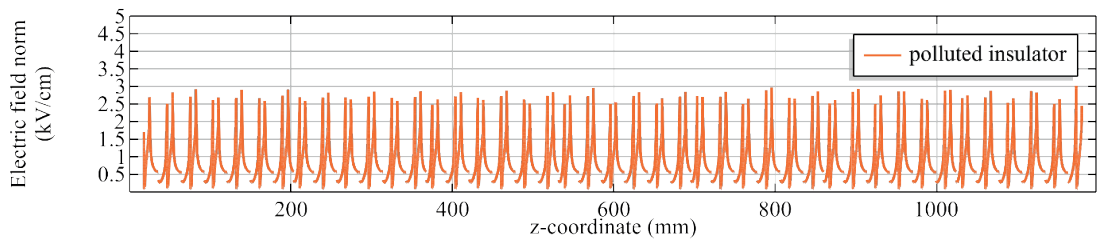
This similarity is even more evident when we look at the stresses on the surface of the silicone rubber, as shown in figure 14.a for the clean insulator and 14.b for the polluted one. In the first case, the mechanical stress approaches 500 Pa at the charged terminal, and is attenuated deeply in its extension, and increases again at the grounded terminal. In the second case, all equipment sheds, including those at the terminals, suffer a stress of 4 to 6 Pa on their surfaces. The pollution layer, in addition to redistributing the efforts, also considerably attenuates them in the insulating electrodes.

In order to more clearly assess each part of the surface, figure 15 shows the stress tensor (red arrows) acting on specific points of the polymer, pointing out its orientation and with each arrow having a size proportional to its magnitude (scale factor: 1). It is clear from the figure that the greatest stress is located at the sheath/shed transition. It is also clear that the stress at this point compresses the shed towards its center.

Figure 16 shows the tracing of the Maxwell stress tensor along the length of the surface of one of the sheds, this one also represented behind the graph, allowing the identification of the curvatures in which the efforts are most intensely manifested. Complementing what is indicated by figure 14. The top of the polluted

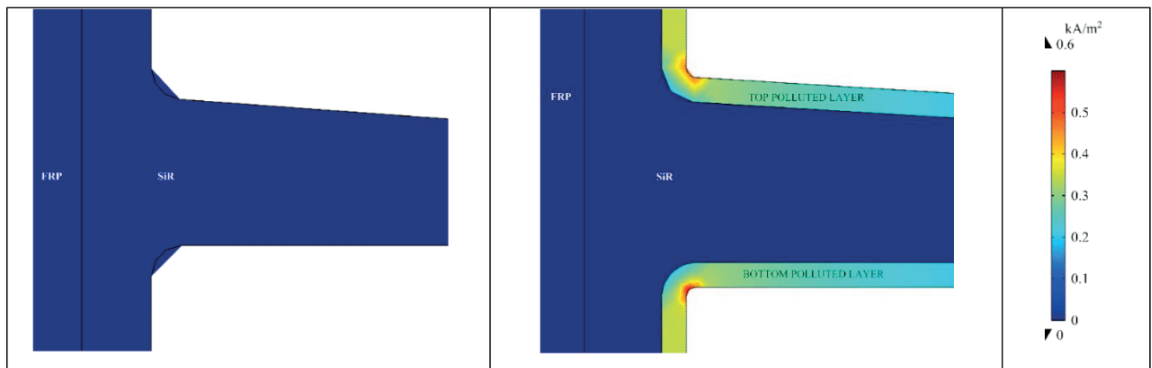


(a)



(b)

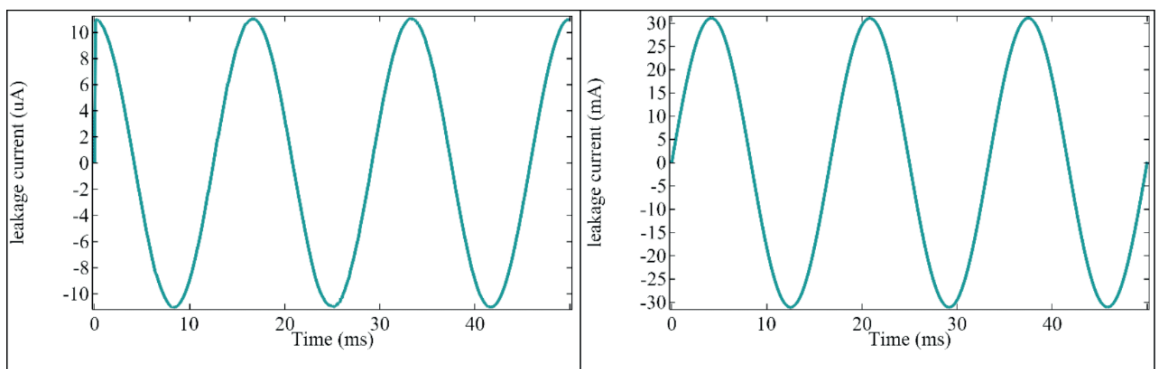
Fig. 10 - Electric field on silicone rubber surface for clean(a) and polluted(b) insulator.



(a) Clean insulator

(b) Polluted insulator

Figure 11: Current density on silicone rubber surface for clean(a) and polluted(b) insulator.



(a) Clean insulator

(b) Polluted insulator

Figure 12: Leakage current on silicone rubber surface for clean(a) and polluted(b) insulator.

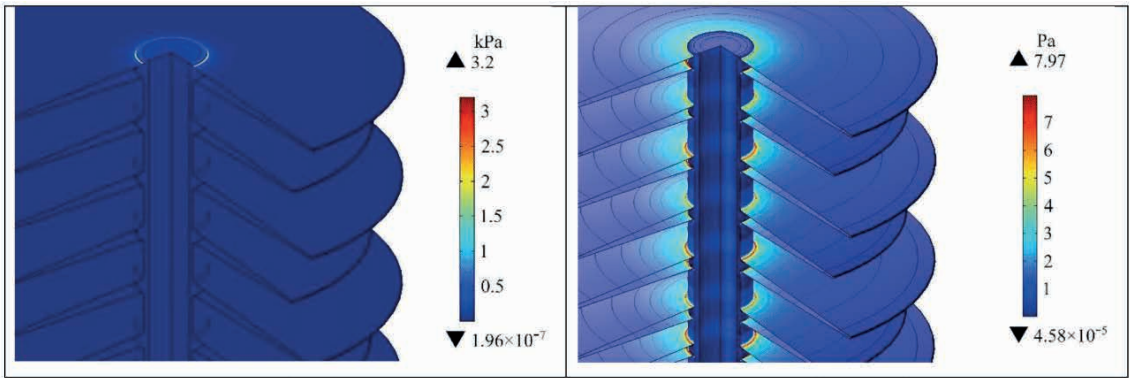
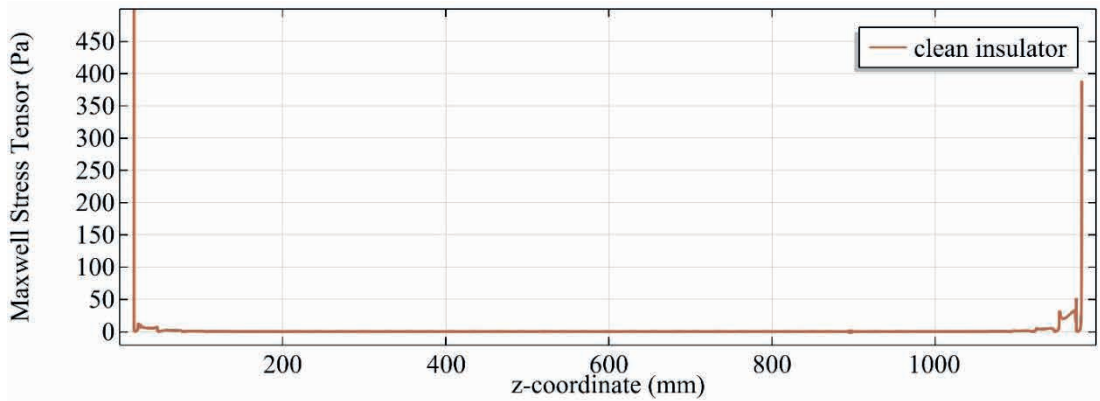
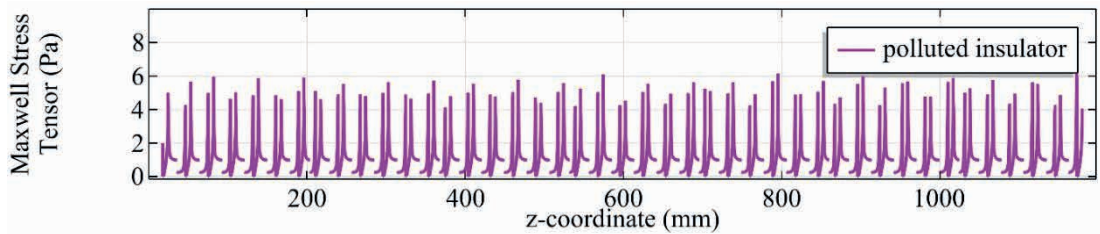


Figure 13: Maxwell stress tensor for clean(a) and polluted(b) insulator.



(a)



(b)

Figure 14: Maxwell stress tensor in SiR surface along the z-axis for clean insulator(a) and polluted insulator(b).

surface is the most affected. While the tip of the disk presents a sharp drop in stress values, growing again when close to the other curvature.

C. DISTRIBUTION OF MAXWELL STRESS ON A CRACK ON THE INSULATOR SHEATH

The evaluative model for a crack-type fault is elucidated in figure 6. This curvilinear region was previously shown to be the one that stores the most electric field in its interior in front of the pollutant layer. Furthermore, insulators removed from service due to electrical failure and available for study at the local laboratory had cracks in the same radial region, as shown in Figure 7, reinforcing the choice for the crack model. With this defect, along the polymer surface there is more stress at the edge of the crack, as shown in Figure 17.

It can be seen from the Figure 17 that the electromechanical stress tensor is directed toward the curvature center. If the force due to this stress overcomes forces that keep the material molecules tied, the crack will move toward the center of the curvature increasing its length and putting the in the risk to be exposed.

D. DISTRIBUTION OF MAXWELL STRESS TENSOR ON A VOID INSIDE THE INSULATOR SHEATH

The simulation of an air bubble inside the polymer as the model shown in Figure 9. The cavity was analyzed at each position of the vertical axis inside the polymeric disk, that is, its central point was displaced from the interface of the bottom of the shed (near to the terminal) to the top interface (opposite the terminal). With this displacement, it became possible to verify the behavior of the electromechanical tensor in the presence of the defect in different regions where it can arise. The graph in Figure 18 demonstrates

the intensity of the stress tensor at four points on the cavity wall as a function of the cavity's vertical position. It can be seen that the stress tensors tend to stretch the cavity in the direction of its center moving the bulk material can in its turn lead to the fibril phenomenon creating new cavities in the material.

CONCLUSION

A FEM model for simulation of electromechanical stress tensor due to leakage current on a polluted insulator was developed, based on this fact some conclusions can be drawn: (i) The polluted insulator has an electric field distribution more homogeneous than the clean insulator; (ii) The model can be applied to estimate the electromechanical stress tensor on polymeric insulators installed on transmission lines of power system; (iii) The internal defect (cavity) tends to be stretched by the electromechanical stress tensor collaborating to the inception of the fibril formation; (iv) The stress tensor can contribute to the increase in cracks on the sheath/shed transition region in the direction of the curvature center increasing the risk of FRP core exposition.

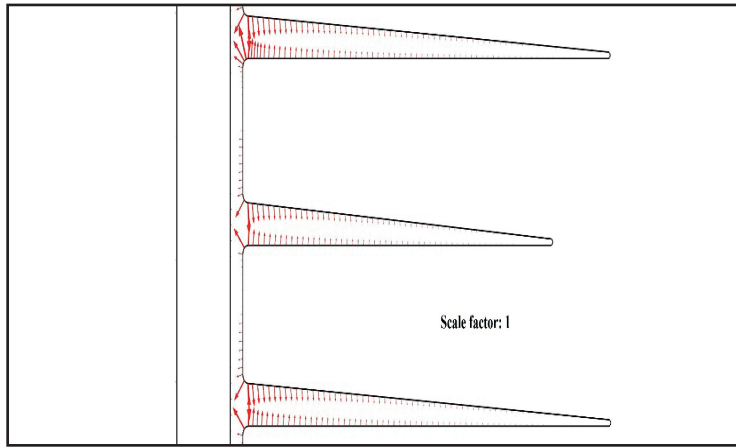


Figure 15: Stress tensor orientation on polluted insulator.

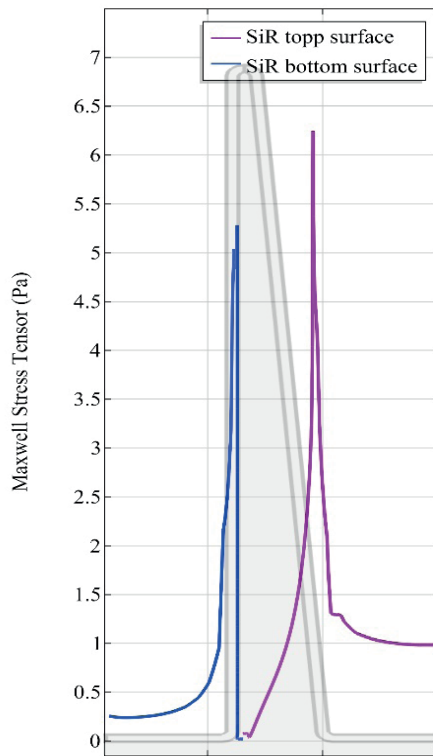


Figure 16: Stress tensor in the shed surface of the SiR.

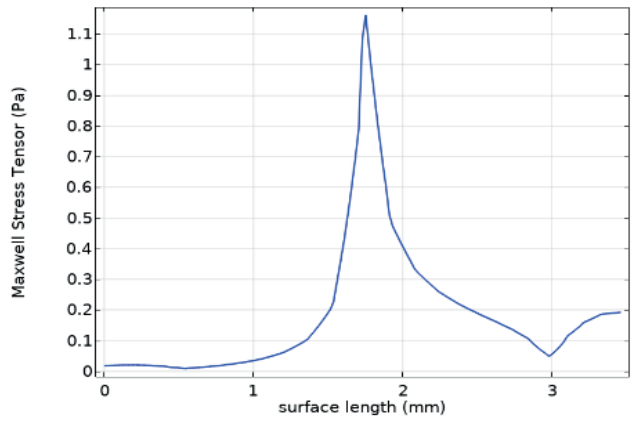
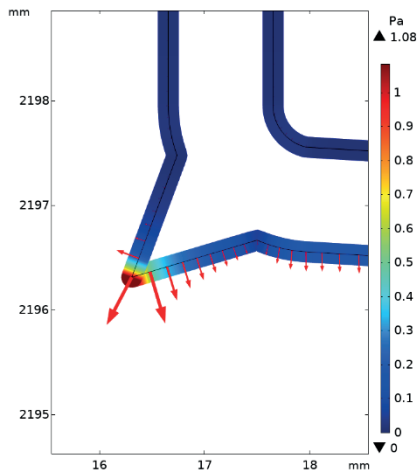


Figure 17: Stress tensor caused by a leakage current of 30 mA at the tip of a crack on the surface of the SiR.

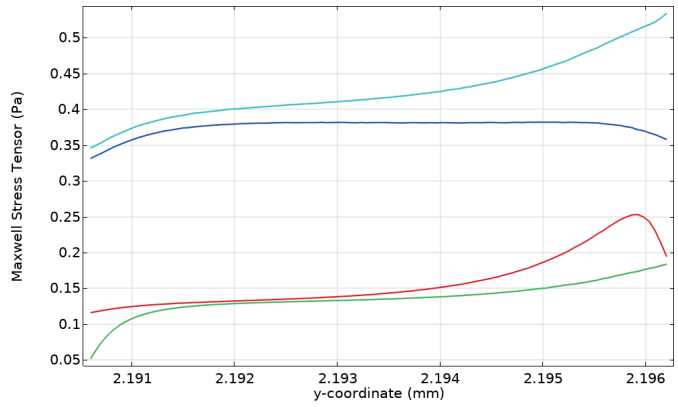
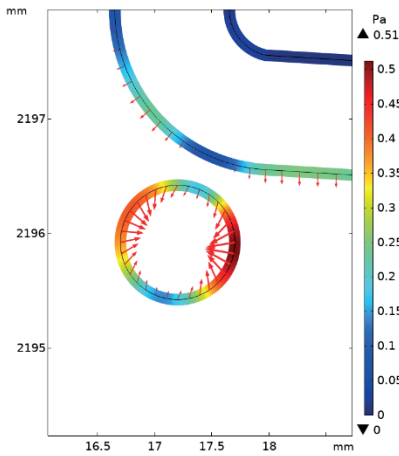


Figure 18: Stress tensor caused by a leakage current of 30 mA in a void inside the SiR housing.

REFERENCES

- [1] Bezerra, R. D. C., Tostes, J. A. S., Teixeira Jr, J. M. T., & Leite, R. C. (2010). Estudo para aumento da confiabilidade de isoladores poliméricos nas linhas de transmissão da Eletronorte. Presented on the III Simpósio Brasileiro de Sistemas Elétricos, Belém, Brasil.
- [2] Kumosa, L. S., Kumosa, M. S., & Armentrout, D. L. (2005). Resistance to brittle fracture of glass reinforced polymer composites used in composite (nonceramic) insulators. *IEEE transactions on power delivery*, 20(4), 2657-2666.
- [3] Farzaneh, M., & Chisholm, W. A. (2009). *Insulators for icing and polluted environments* (Vol. 47). John Wiley & Sons.
- [4] Ravi, K. N., & Vasudev, N. (2017, January). Experimental study on surface erosion and brittle fracture of FRP rod in polymeric insulators. In *National Conference on High Voltage Engineering & Technology (NCHVET2017)* (Vol. 27, p. 28).
- [5] Wang, Jiafu, Xidong Liang, and Yanfeng Gao. "Failure analysis of decay-like fracture of composite insulator." *IEEE Transactions on Dielectrics and Electrical Insulation* 21.6 (2014): 2503-2511.
- [6] Gao, Y., Liang, X., Bao, W., Li, S., & Wu, C. (2018). Failure analysis of a field brittle fracture composite insulator: characterization by FTIR analysis and fractography. *IEEE Transactions on Dielectrics and Electrical Insulation*, 25(3), 919-927.
- [7] Gao, Y., Liang, X., Bao, W., Wu, C., & Li, S. (2019). Failure analysis of a field brittle fracture composite insulator: characterisation by X-ray photoelectron spectroscopy analysis. *High Voltage*, 4(2), 89-96.
- [8] Chughtai, Abdul R., et al. "FTIR analysis of non-ceramic composite insulators." *IEEE transactions on dielectrics and electrical insulation* 11.4 (2004): 585-596.
- [9] Verma, Alok Ranjan, and B. Subba Reddy. "Accelerated aging studies of silicon-rubber based polymeric insulators used for HV transmission lines." *Polymer Testing* 62 (2017): 124-131.
- [10] Fourmigue, J. M., M. Noel, and G. Riquel. "Aging of polymeric housing for HV insulators: comparison between natural and artificial testing." *Proceedings of 1995 Conference on Electrical Insulation and Dielectric Phenomena*. IEEE, 1995.
- [11] Gorur, Ravi S., et al. "Aging in silicone rubber used for outdoor insulation." *IEEE Transactions on Power Delivery* 7.2 (1992): 525-538.
- [12] Kumagai, S., and N. Yoshimura. "Polydimethylsiloxane and alumina trihydrate system subjected to dry-band discharges or high temperature part I: chemical structure." *IEEE transactions on dielectrics and electrical insulation* 11.4 (2004): 691-700.
- [13] Chakraborty, Rahul. "Performance of silicone rubber insulators under thermal and electrical stress." *IEEE Transactions on Industry Applications* 53.3 (2017): 2446-2454.
- [14] Shaik, Mohamed Ghouse, and Vijayarekha Karuppaiyan. "Investigation of surface degradation of aged high temperature vulcanized (HTV) silicone rubber insulators." *Energies* 12.19 (2019): 3769.
- [15] Verma, A. R., Reddy, G. S., & Chakraborty, R. (2018). Multistress aging studies on polymeric insulators. *IEEE Transactions on Dielectrics and Electrical Insulation*, 25(2), 524-532.
- [16] Kinloch, A. J. (Ed.). (2013). *Fracture behaviour of polymers*. Springer Science & Business Media.
- [17] Anderson, T. L. (2017). *Fracture mechanics: fundamentals and applications*. CRC press.
- [18] Stratton, J. A. (2007). *Electromagnetic theory* (Vol. 33). John Wiley & Sons.
- [19] Multiphysics, C., Guide, A. M. U. S., & Comsol AB Group. (2010). Burlington.

- [20] Landau, L. D., Bell, J. S., Kearsley, M. J., Pitaevskii, L. P., Lifshitz, E. M., & Sykes, J. B. (2013). *Electrodynamics of continuous media* (Vol. 8). elsevier.
- [21] Melcher, J. R. (1981). *Continuum electromechanics* (Vol. 2). Cambridge, MA: MIT press.
- [22] Farzaneh, M., & Chisholm, W. A. (2009). *Insulators for icing and polluted environments* (Vol. 47). John Wiley & Sons.
- [23] Nekahi, A., McMeekin, S. G., & Farzaneh, M. (2015, July). Effect of pollution severity on electric field distribution along a polymeric insulator. In 2015 IEEE 11th international conference on the properties and applications of dielectric materials (ICPADM) (pp. 612-615). IEEE.
- [24] Miller, H. C. (1989). Surface flashover of insulators. *IEEE transactions on electrical insulation*, 24(5), 765-786.
- [25] Ahmadi-Joneidi, I., Shayegani-Akmal, A. A., & Mohseni, H. (2017). Leakage current analysis of polymeric insulators under uniform and non-uniform pollution conditions. *IET Generation, Transmission & Distribution*, 11(11), 2947-2957.
- [26] IEC/TS – 60815 Selection And Dimensioning Of High-Voltage Insulators Intended For Use In Polluted Conditions – Part 1.
- [27] Hall, J. F., & Paul, T. (1981). Wind tunnel studies of the insulator contamination process. *IEEE Transactions on Electrical Insulation*, (3), 180-188.
- [28] Lewis, T. J., Llewellyn, J. P., Van der Sluijs, M. J., Freestone, J., & Hampton, R. N. (1996, September). A new model for electrical ageing and breakdown in dielectrics. In Seventh International Conference on Dielectric Materials, Measurements and Applications (Conf. Publ. No. 430) (pp. 220-224). IET.
- [29] Stratton, J. A. (2007). *Electromagnetic theory* (Vol. 33). John Wiley & Sons.
- [30] T. Bai and P. L. Lewin, "Degradation behaviour of voids in silicone rubber under applied AC electric fields," 2012 Annual Report Conference on Electrical Insulation and Dielectric Phenomena, 2012, pp. 589-592, doi: 10.1109/CEIDP.2012.6378849.